Available online at www.sciencedirect.com
ScienceDirect
Toxicology and Applied Pharmacology 220 (2007) 45 – 59
Toxicology and Applied Pharmacology
www.elsevier.com/locate/ytaap

# Gene expression profiles of murine fatty liver induced by the administration of valproic acid

Min-Ho Lee [a,b], Il Hong [a,b], Mingoo Kim [c,h], Byung Hoon Lee [a,h], Ju-Han Kim [c,h], Kyung-Sun Kang [d,h], Hyung-Lae Kim [e,h], Byung-Il Yoon [f,h], Heekyoung Chung [g,h], Gu Kong [g,h], Mi-Ock Lee [a,b,h,*]

[a] *College of Pharmacy, Republic of Korea*
[b] *Bio-MAX Institute, Republic of Korea*
[c] *Seoul National University Biomedical Informatics College of Medicine, Republic of Korea*
[d] *Department of Veterinary Public Health College of Veterinary Medicine, Seoul National University, Seoul 151-742, Republic of Korea*
[e] *Department of Biochemistry College of Medicine, Ewha Womans University, Seoul 158-710, Republic of Korea*
[f] *School of Veterinary Medicine, Kangwon National University, Kangwon 200-701, Republic of Korea*
[g] *Department of Pathology College of Medicine, Republic of Korea*
[h] *Toxicogenomics Research Consortium, Hanyang University, Seoul 133-791, Republic of Korea*

Received 4 October 2006; revised 13 December 2006; accepted 13 December 2006
Available online 22 December 2006

**Abstract**

Valproic acid (VPA) has been used as anticonvulsants, however, it induces hepatotoxicity such as microvesicular steatosis and necrosis in the liver. To explore the mechanisms of VPA-induced steatosis, we profiled the gene expression patterns of the mouse liver that were altered by treatment with VPA using microarray analysis. VPA was orally administered as a single dose of 100 mg/kg (low-dose) or 1000 mg/kg (high-dose) to ICR mice and the animals were killed at 6, 24, or 72 h after treatment. Serum alanine aminotransferase and aspartate aminotransferase levels were not significantly altered in the experimental animals. However, symptoms of steatosis were observed at 72 h with low-dose and at 24 h and 72 h with high-dose. After microarray data analysis, 1910 genes were selected by two-way ANOVA ($P<0.05$) as VPA-responsive genes. Hierarchical clustering revealed that gene expression changes depended on the time rather than the dose of VPA treatment. Gene profiling data showed striking changes in the expression of genes associated with lipid, fatty acid, and steroid metabolism, oncogenesis, signal transduction, and development. Functional categorization of 1156 characteristically up- and down-regulated genes (cutoff >1.5-fold) revealed that 60 genes were involved in lipid metabolism that was interconnected with biological pathways for biosynthesis of triglyceride and cholesterol, catabolism of fatty acid, and lipid transport. This gene expression profile may be associated with the known steatogenic hepatotoxicity of VPA and it may provide useful information for prediction of hepatotoxicity of unknown chemicals or new drug candidates through pattern recognition.


*Keywords:* Valproic acid; Toxicogenomics; Microarray analysis; Fatty liver

## Introduction

Valproic acid (VPA) is an eight-carbon branched-chain fatty acid with anticonvulsant properties. VPA has been used clinically for epilepsy for years, as the second major treatment option discovered after lithium (Bowden, 2003). VPA is also being tested as a chemotherapeutic agent based on recent preclinical evidence of its anticancer activity (Blaheta and Cinatl, 2002). VPA inhibits the proliferation and differentiation of malignantly transformed cells (Gottlicher et al., 2001). This effect is likely to be associated with the inhibition of histone deacetylase activity (Gurvich et al., 2004).

During the clinical trials of VPA, various side effects have been reported, such as convulsions, facial edema, lassitude, hypoglycemia, and vomiting (Powell-Jackson et al., 1984; Schmidt, 1984). Among these, hepatotoxicity is considered the most serious. Type I hepatotoxicity is associated with dose-

* Corresponding author. Fax: +82 2 8872692.
*E-mail address:* molee@snu.ac.kr (M.-O. Lee).

0041-008X/$ - see front matter © 2006 Elsevier Inc. All rights reserved.
doi:10.1016/j.taap.2006.12.016

dependent changes in the serum levels of liver enzymes and low plasma fibrinogen levels, which occur within the first 3 months of therapy in about 20% of patients. Type II hepatotoxicity is rare, but often fatal. It is an irreversible idiosyncratic reaction characterized by microvesicular steatosis, which is sometimes accompanied by necrosis (Tong et al., 2005). Hepatic steatosis has also been observed in experimental animals: an intradermal injection of 750 mg/kg sodium valproate induced significant microvesicular steatosis after 48 h in rats (Lewis et al., 1982). Microvesicular steatosis with accompanying necrosis and infiltration was observed in 13% of mice injected intraperitoneally with sodium valproate at varying doses from 50 to 800 mg/kg (Roma-Giannikou et al., 1999). Although the mechanism underlying VPA-induced hepatotoxicity has not been fully elucidated, reactive VPA metabolites, *i.e.*, 4-ene-VPA, and its subsequent metabolite, (*E*)-2,4-diene-VPA, may be involved in the inhibition of mitochondrial fatty acid β-oxidation (Kesterson et al., 1984; Ponchaut et al., 1992; Kassahun and Abbott, 1993).

Drug-induced hepatotoxicity is an important healthcare issue because it causes significant morbidity and mortality, and can be extremely difficult to predict (Kaplowitz, 2001). Therefore, evaluating the mechanisms of drug-induced hepatotoxicity is important and necessary for the design of safer therapeutic agents. Microarray technology has been applied in toxicology field to understand the mechanisms of drug-induced toxicity, to identify biomarkers, and to predict toxicity of chemicals (Gunther et al., 2003; Searfoss et al., 2003; Vrana et al., 2003). Previous studies have approached profiling of gene expression changes that induced VPA to elucidate its mechanism of action as a mood-stabilizing agent, and to understand its adverse effects such as teratogenicity and hepatotoxicity (Glauser et al., 2003; Kultima et al., 2004, Bosetti et al., 2005; Jolly et al., 2005; Schnackenberg et al., 2006). However, some of the previous results were contradictory, and some were not comparable because of different experimental conditions such as different VPA administration protocols, experimental animals, tissues, and microarray tools used. In the present investigation, therefore, we aimed to obtain gene expression profiling for the VPA-induced murine fatty liver, which was accompanied by apparent histopathological changes in microvesicular steatosis. Our gene expression profiling data showed significant changes in the expression of genes that are important in lipid transport, triglyceride and cholesterol biosynthesis, and fatty acid oxidation. This information would be used as a tool to predict toxicity of unknown chemicals or new drug candidates, which will eventually contribute to improve the processes of risk assessment and safety evaluation.

## Materials and methods

*Animals and study design.* Male ICR mice, 6 weeks of age, were obtained from Japan SLC Inc. (Hamamatsu, Japan). The mice were housed five per cage in polycarbonate cages, and commercial mouse chow (Certified Rodent Diet 5002; Purina Mills Inc., St Louis, MO) and water were supplied *ad libitum.* The animal laboratory was located at the Animal Center for Pharmaceutical Research, College of Pharmacy, Seoul National University (Seoul, Korea). It was maintained at a temperature of 20 °C to 23 °C, and humidity of 30% to 48%, with 12-h light/dark cycle. Upon arrival at the animal laboratory, the mice were allowed at least 4 days to acclimatize. Food was withdrawn for 4 h before and was resupplied 2 h after VPA administration. Sodium valproate was obtained from Sigma Chemical Co. (St Louis, MO) and dissolved in distilled water. Mice ($n=3$) were dosed by oral gavage with 100 mg/kg (*low-dose*) or 1000 mg/kg VPA (*high-dose*), and killed at 6, 24, or 72 h after drug treatment. Distilled water was administered to the vehicle-treated control groups. The doses of 100 mg/kg and 1000 mg/kg were selected by range-finding studies. High-dose was determined as a minimal dose that induced microvesicular steatosis at 24 h of treatment. To compare with human therapeutic doses, 20 to 30 mg/kg/day, a relatively high dose was required to induce steatosis in mice, which may be due to different half-life of VPA in species, *i.e.*, 0.8 h in mice and 20 h in humans (Loscher, 1978, 1999).

*Clinical chemistry and histopathology.* For the analysis of serum liver enzymes, animals were euthanized with diethyl ether and blood was drawn from the inferior vena cava. Serum alanine aminotransferase (ALT) and aspartate aminotransferase (AST) activities were measured with the Prestige 24i fully automated biochemical analyzer (Tokyo Boeki Pty Ltd, Tokyo, Japan) at the Department of Pathology, Korea Food and Drug Administration (Seoul, Korea). For microarray analysis, a cross-section of the left lobe of the liver was collected in an RNase-free tube containing RNAlater (Ambion, Austin, TX). The RNAlater-permeated tissues were kept overnight at 4 °C and then stored at −20 °C until use. For histopathological analysis, cross-sections of the left, median, right anterior, right posterior and caudate lobes were collected and fixed in 10% neutral buffered formalin. The fixed liver tissues were dehydrated, embedded in paraffin, sectioned to 5 μm thicknesses, and processed for hematoxylin and eosin (H&E) staining. Histopathological examination of the liver sections was conducted by a pathologist and peer-reviewed.

*RNA isolation.* Total RNA was isolated from the RNAlater-permeated cross-sections of the left lobe using easy-BLUE (iNtRON Biotechnology Inc., Sungnam, Korea), and was purified using an RNeasy Mini Kit (Qiagen, Valencia, CA). The concentration and purity of the total RNA were determined by spectrophotometry and its quality was determined by gel analysis using RNA Nano LabChip® on an Agilent 2100 Bioanalyzer (Agilent Technologies, Palo Alto, CA).

*Microarray analysis.* Applied Biosystems Mouse Genome Survey Arrays (Applied Biosystems, Foster City, CA), which contain 60-mer oligonucleotide probes representing a set of 32996 individual mouse genes and more than 1000 control probes, were used for this investigation. Digoxigenin (DIG)–UTP-labeled cRNA was generated from 5 μg of total RNA and linearly amplified using a chemiluminescent reverse transcription (RT) *in vitro* transcription labeling kit (Applied Biosystems). Briefly, each microarray was prehybridized in hybridization buffer with blocking reagent at 55 °C for 1 h. Digoxigenin-labeled cRNA targets (10 μg) were fragmented to 100–400 bp and hybridized with each prehybridized microarray at 55 °C for 16 h. The arrays were washed with hybridization wash buffer and then with chemiluminescence rinse buffer. Chemiluminescent signals were generated by incubating the arrays serially with anti-DIG–alkaline phosphatase and chemiluminescence substrate. Synthetic bacterial control genes (*Dap*, *Lys*, *Phe*, *BioB*, *BioC*, and *BioD*), DIG-labeled oligonucleotides, and LIZ® fluorescent-dye-labeled 24-mer oligonucleotides, were used as the quality controls for the microarray analysis. Images were collected for each microarray using the 1700 Chemiluminescent Microarray Analyzer (Applied Biosystems). Microarray images were auto-gridded and the chemiluminescent signals were quantified, corrected for background, spatially normalized, and exported for a quality report. Microarray data with quality reports above the manufacturer's threshold were used for further analysis.

*Data analysis.* The assay signal and the assay signal-to-noise ratio values for the microarray images were extracted using Applied Biosystems Expression System software. Bad spots flagged by the software (flag <100) were removed from the analysis. The assay signals of the probe sets were imputed by a KNN imputation algorithm (Troyanskaya et al., 2001), variance stabilization transformed (Huber et al., 2002) and quantile normalized (Bolstad et al., 2003). Differentially expressed probe sets were selected by two-way ANOVA ($P<0.05$). Gene sets with different dose and time effects according to two-way ANOVA were classified into time-dependent (MTx), dose-dependent (MxD),

Table 1
Primer sequences used for validation of the microarray analysis by semi-quantitative RT–PCR

| Gene | RefSeq | Nucleotide sequence | | Annealing temperature (°C) | Number of cycles |
|---|---|---|---|---|---|
| *Gsta2* | NM_008182 | Sense | 5′-CAGGGGTGGAGTTTGAAGAGA-3′ | 59 | 30 |
| | | Antisense | 5′-CCCACAAGGTAGTCTTGTCCA-3′ | | |
| *Fkbp5* | NM_010220 | Sense | 5′-GAAGATTCAGGCGTTATCCGTA-3′ | 59 | 25 |
| | | Antisense | 5′-TTGCCTCCCTTGAAGTACACA-3′ | | |
| *Fgf21* | NM_020013 | Sense | 5′-CAAGCATACCCCATCCCTGA-3′ | 59 | 25 |
| | | Antisense | 5′-GGTTTGGGGAGTCCTTCTGA-3′ | | |
| *Fmo3* | NM_008030 | Sense | 5′-AGAACTCAGCCATGTAGCTCA-3′ | 59 | 30 |
| | | Antisense | 5′-TAGAGTCATCCAGGAAGGGGTA-3′ | | |
| *Cyp1b1* | NM_009994 | Sense | 5′-CCAGCCAGGACACCCTTTCCA-3′ | 59 | 30 |
| | | Antisense | 5′-ACCTCCGTTTGCCCACTGAGA-3′ | | |
| *LOC277830* | NM_201640 | Sense | 5′-AACTTGCCCATGATCACACA-3′ | 58 | 25 |
| | | Antisense | 5′-TGACCTGGACACCTTTAGGTA-3′ | | |
| *Cyp4a14* | NM_007822 | Sense | 5′-GTCCTGCTTTATGATCCTGA-3′ | 55 | 25 |
| | | Antisense | 5′-CAGGTTGTTTAGATCCTCGA-3′ | | |
| *H2-Ea* | NM_010104 | Sense | 5′-CACTGGCTAATATAGCTGTGGA-3′ | 58 | 30 |
| | | Antisense | 5′-CATGATGAGGATAATCCCCACA-3′ | | |
| *Hspa2* | NM_008301 | Sense | 5′-GGATGGCATCTTTGAGGTGA-3′ | 58 | 30 |
| | | Antisense | 5′-ATCTTGCAGGAGCTTCTGGA-3′ | | |
| *β-actin* | X03672 | Sense | 5′-CGTGGGCCGCCCTAGGCACCA-3′ | 58 | 25 |
| | | Antisense | 5′-TTGGCTTAGGGTTCAGGGGGG-3′ | | |

and combined effect (MTD) groups. The three groups were then classified into with- and without-interaction groups according to the significance of the interaction terms under saturated linear models. Hierarchical and *K*-means clustering were applied to the differentially expressed genes using the Multiexperiment Viewer software (Saeed et al., 2003; http://www.tm4.org). Genes were annotated and biological processes were analyzed by Protein ANalysis THrough Evolutionary Relationships (PANTHER) (Mi et al., 2005; http://www.pantherdb.org). The biological pathways were analyzed with Kyoto encyclopedia of genes and genomes (KEGG) pathway analysis (Ogata et al., 1999; http://www.genome.ad.jp/kegg/genes.html).

*Reverse transcription–polymerase chain reaction (RT–PCR).* To confirm the changes in gene expression identified using the oligonucleotide microarray, semi-quantitative RT–PCR was performed. Total RNA was obtained from the individual liver section that was randomly selected from each experimental group ($n=3$). RT was performed with 4 μg of total RNA and 4 μg of random hexamer (Amersham Biosciences, Sweden) using Moloney murine leukemia virus reverse transcriptase (Invitrogen, Carlsbad, CA). The resulting cDNA was stored at −20 °C until use. PCR were performed with *i-taq* DNA polymerase (iNtRON Biotechnology Inc.) using an MJ Research PTC 200 thermal cycler (Reno, NV). The primers and conditions for PCR are listed in Table 1. The genes were analyzed under conditions in which PCR products were exponentially amplified.

## Results

### *Clinical chemistry and histopathology*

VPA was administered to male ICR mice orally at a dose of 100 mg/kg (low-dose) or 1000 mg/kg (high-dose) for 6, 24, or 72 h. Hepatotoxicity was evaluated from serum ALT and AST levels (Fig. 1A). No significant changes were observed between

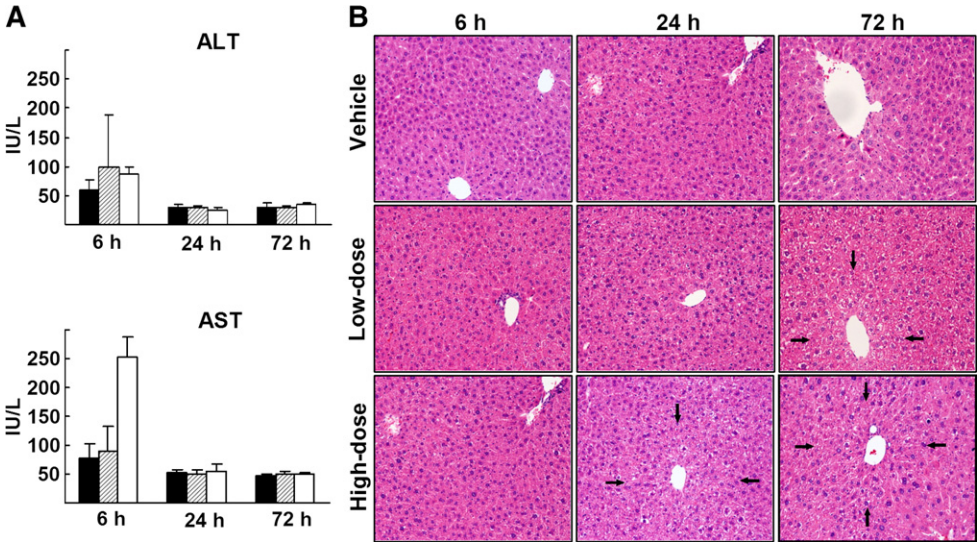


Fig. 1. Assessment of hepatotoxicity induced by VPA. (A) Serum levels of AST and ALT. ■, Vehicle-treated control; ▧, low-dose VPA; and □, high-dose VPA. Results are means ($n=3$)±SD. (B) Histological assessment of livers. Photomicrographs of H&E-stained samples (200× magnification).

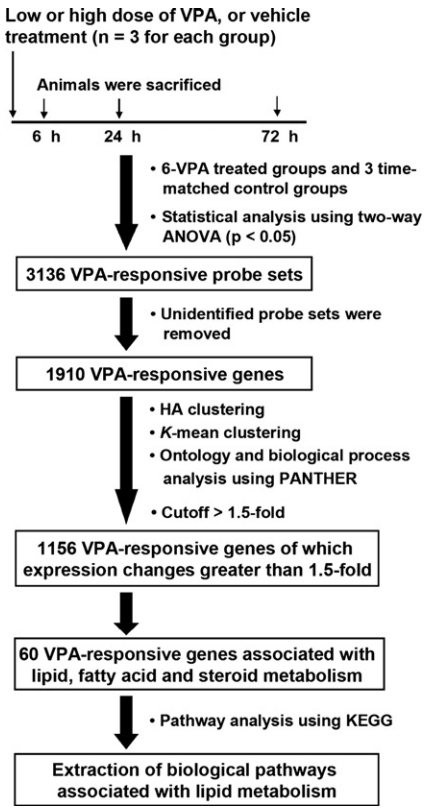


Fig. 2. Schematic representation of the experimental design and data analysis flow chart for this microarray experiment.

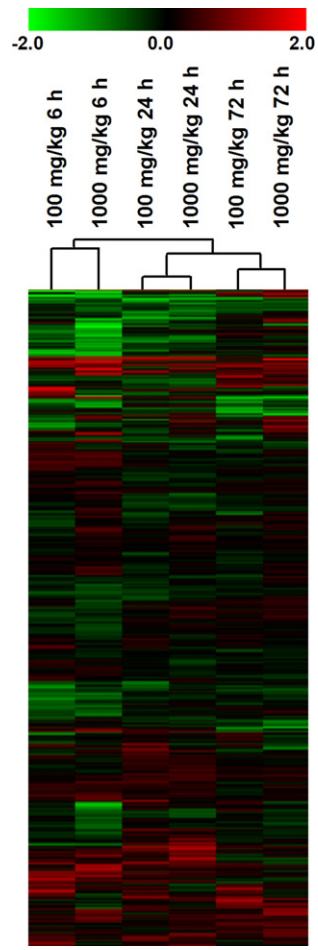


Fig. 4. Hierarchical clustering of 1910 genes that showed differential expression patterns. The genes were clustered by Euclidean distance. The *y*-axis of the dendrogram represents the gene symbol, but these have been deleted for simplicity. The *x*-axis represents the various times and doses of VPA treatments and expression intensities relative to those of time-matched controls (fold change in $\log_2$ values) are given in color: green for down-regulation, red for up-regulation, and black for insignificant changes.

VPA-treated groups and vehicle-treated control groups, except for a significant increase in AST levels after high-dose treatment for 6 h. All the values for the VPA-treated groups and vehicle-treated control groups were within the normal reference ranges, *i.e.*, ALT, 28–184 IU/L and AST, 55–261 IU/L (Canadian Council on Animal Care; http://www.ccac.ca/en/CCAC_Main.htm). However, H&E staining of the liver sections obtained from the VPA-treated groups showed dose- and time-dependent fatty changes around the central vein. Fatty changes were observed after 72 h treatment with low-dose and after 24 h and

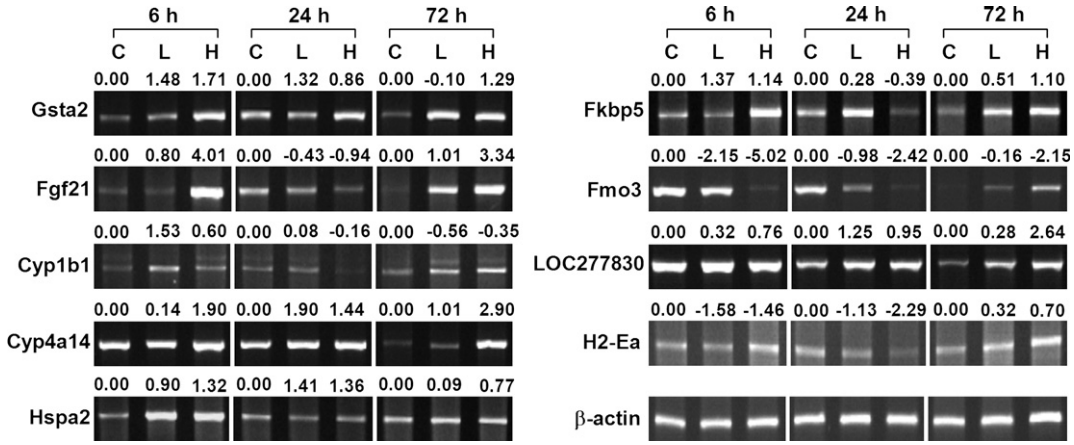


Fig. 3. Differential expression levels of selected genes determined by microarray and RT–PCR analyses. The mean fold changes in expression levels ($n=3$) measured by microarray analysis are shown at the top of the gel illustrations. RT–PCR was performed using randomly selected RNA samples from each experimental group. The experiments were repeated at least three times and representative figures are shown. C, vehicle-treated control; L, low-dose VPA; H, high-dose VPA.

72 h treatment with high-dose. Representative stained samples of liver sections are shown in Fig. 1B. Together, these data indicate that VPA induces lipid accumulation in the liver without marked changes in serum liver enzyme levels under our experimental conditions.

*Gene expression analysis*

To identify global gene expression changes associated with VPA-induced hepatotoxicity, microarray analysis was performed using Applied Biosystems Mouse Genome Survey Arrays. Transcript profiling was performed separately on three individual liver sections in six VPA-treated groups and three time-matched vehicle-treated control groups, generating a total of 27 microarray data sets. We used a multistep method to analyze the microarray gene expression data (Fig. 2). First, the transformed and normalized data were subjected to two-way ANOVA, and 3136 probe sets were identified as significantly altered in their expression levels ($P<0.05$) (Supplementary Table 1). After unknown probe sets were removed, 1910 probe sets were considered to represent VPA-responsive genes (Supplementary Table 2). The numbers of up-regulated and down-regulated genes were similar in the data sets for six experimental time points. For example, 912 genes were up-regulated and 998 genes were down-regulated in the group of low-dose VPA treatment for 72 h, and 976 genes were up-regulated and 934 genes were down-regulated in the group of high-dose treatment for 24 h. The genes were classified into four groups under the terms of a saturated linear model: 1222 of 1910 differentially expressed genes showed a time-dependent response (MTx), 323 genes were dose-dependent (MxD), and 181 genes were both time- and dose-dependent (MTD). To verify the gene expression profiles detected with the oligonucleotide microarray, nine genes that showed significant changes in expression were selected and subjected to semi-quantitative RT–PCR analysis. The semi-quantitative RT–PCR and microarray results were quite compatible at each time point: 7/9 (77.8%) at 6 h, 7/9 (77.8%) at 24 h, and 7/9 (77.8%) at 72 h showed the same patterns of change (Fig. 3).

Next, we performed hierarchical clustering of the 1910 VPA-responsive genes. As shown in Fig. 4, the differentially expressed genes were clustered according to the similarity of their expression patterns by dose and time of treatments. Low- and high-dose treated groups at each time point were in the same node and the distance between nodes increased in response to the treated time, indicating that the treated time influenced strongly than the dose of VPA in this experiment. This profile also indicates that there are two distinct phases of gene expression changes, *i.e.*, early phase at 6 h and late phase at 24 h and 72 h, suggesting that VPA induces a dynamic and complex program of gene regulatory events during the onset of fatty liver.

Table 2
Significant PANTHER biological process terms for the VPA-responsive genes [a]

| Biological process | *p* value | Biological process | *p* value |
|---|---|---|---|
| Oncogenesis | 2.03e−05 | Apoptosis | 5.34e−02 |
| Gametogenesis | 1.48e−03 | DNA replication | 5.41e−02 |
| Lipid and fatty acid transport | 2.48e−03 | Homeostasis | 5.60e−02 |
| mRNA splicing | 4.67e−03 | Oxidative phosphorylation | 5.64e−02 |
| Oncogene | 5.22e−03 | Amino acid activation | 5.67e−02 |
| DNA metabolism | 6.10e−03 | Synaptic transmission | 6.69e−02 |
| Tumor suppressor | 6.87e−03 | Other coenzyme and prosthetic group metabolism | 6.70e−02 |
| Pre-mRNA processing | 8.73e−03 | Other signal transduction | 7.57e−02 |
| Interferon-mediated immunity | 1.30e−02 | Electron transport | 8.11e−02 |
| rRNA metabolism | 1.48e−02 | Transport | 8.18e−02 |
| Protein targeting | 2.36e−02 | Amino acid catabolism | 8.49e−02 |
| DNA repair | 2.69e−02 | Neurotransmitter release | 8.54e−02 |
| Blood circulation and gas exchange | 2.99e−02 | Other blood circulation and gas exchange activity | 8.62e−02 |
| Angiogenesis | 3.07e−02 | Cell structure | 8.73e−02 |
| Proteolysis | 3.11e−02 | Amino acid metabolism | 8.86e−02 |
| Cell motility | 3.29e−02 | Apoptotic processes | 8.93e−02 |
| Chromatin packaging and remodeling | 3.56e−02 | DNA degradation | 8.93e−02 |
| Cell adhesion-mediated signaling | 4.25e−02 | Other oncogenesis | 9.12e−02 |
| Lipid, fatty acid and steroid metabolism | 4.90e−02 | Constitutive exocytosis | 9.36e−02 |
| Oogenesis | 5.02e−02 | Reverse transcription | 9.45e−02 |
| Protein metabolism and modification | 5.07e−02 | Other nucleoside, nucleotide and nucleic acid metabolism | 9.72e−02 |

[a] Shown are PANTHER biological process terms that significantly over-represented (Mann–Whitney *U* test, $P<0.1$) for the VPA-responsive genes.

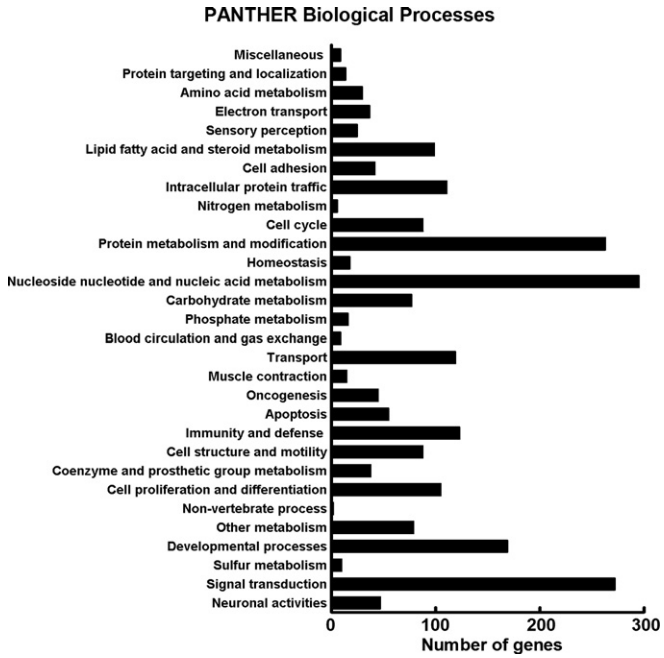


Fig. 5. Gene ontology of the biological processes for the VPA-regulated genes. Analysis of the biological processes in which the VPA-regulated genes were implicated using PANTHER. The numbers of genes in specific biological process annotations are presented.

*Functional classification of differentially expressed genes*

The PANTHER database involves the curator-defined grouping of protein sequences into functional subfamilies, allowing their more detailed and accurate association with ontology terms

and biological pathways (Mi et al., 2005). The 1910 differentially expressed genes were individually annotated and the predominant biological processes represented by these genes were identified using the ontology-driven clustering approach of PANTHER. As shown in Fig. 5, VPA induced changes in the expression of genes involved in biological processes, such as "protein metabolism and modification", "nucleoside, nucleotide, and nucleic acid metabolism" and "signal transduction". Among these, the most statistically significant overrepresented terms included "oncogenesis" and "lipid and fatty acid transport" (Table 2). To gain more insight into the biological functions of these gene products relative to the time and dose of VPA administration, the 1910 genes were divided into six groups using *K*-means clustering analysis, an algorithm that extracts prominent expression patterns from a set of profiles (Steinley, 2006). The pattern of expression changes in clusters, the number of genes belonging to each cluster, and the statistically significant biological processes involved are shown in Fig. 6.

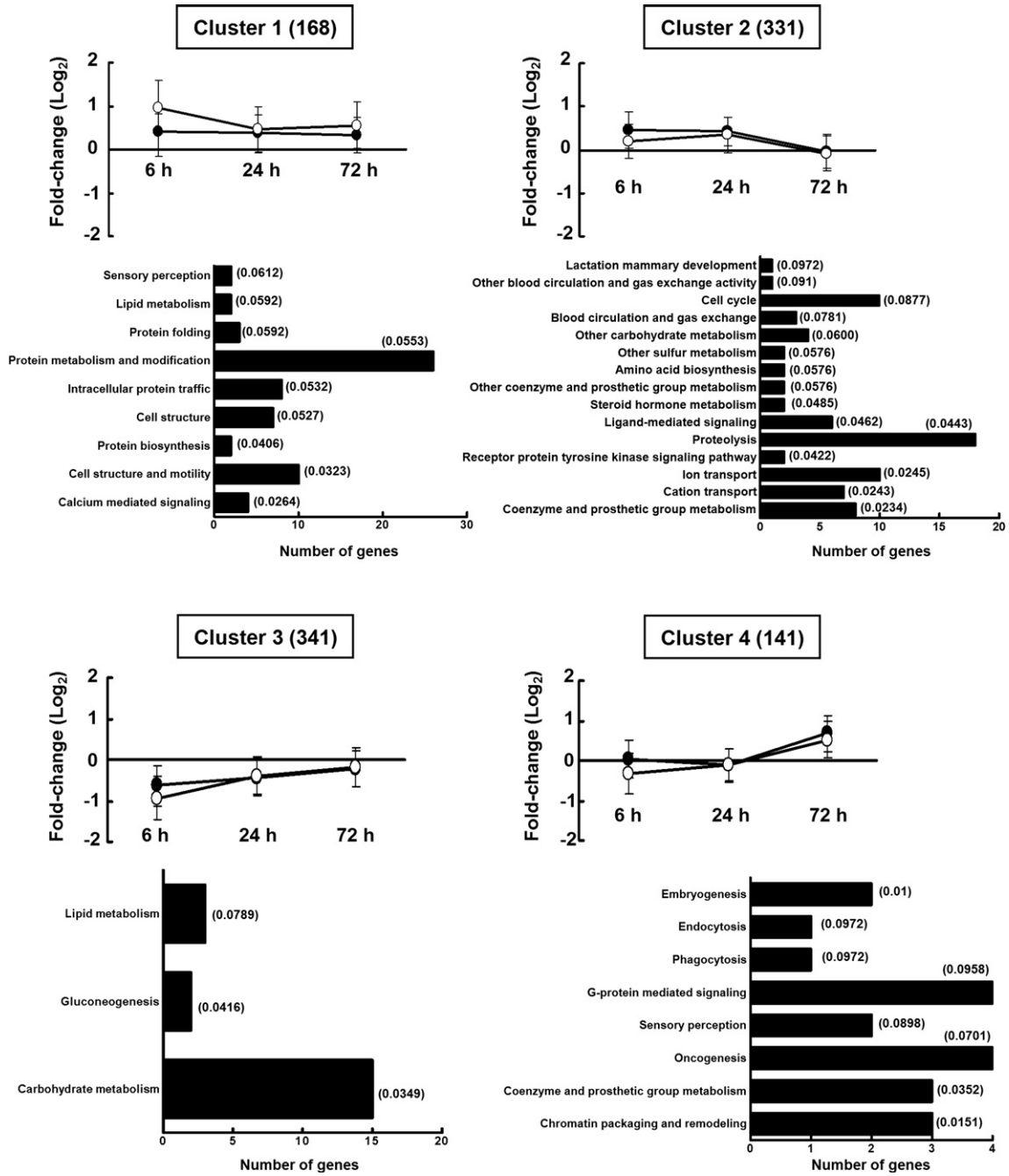


Fig. 6. *K*-means clustering analysis of the genes differentially expressed after VPA administration. *K*-means clustering analysis of 1910 differentially expressed genes produced six clusters. The number of genes belonging to each cluster is given in parentheses. The *y*-axis represents the fold change in expression (VPA-treated vs. vehicle-treated control) on a $\log_2$ scale. The PANTHER gene expression data analysis tool was used to identify statistically significantly overrepresented biological process terms for each cluster (Mann–Whitney *U* test, $P<0.1$). The bar graph indicates the numbers of genes belonging to specific biological process terms. The *P* value for each biological process term is indicated in parentheses.

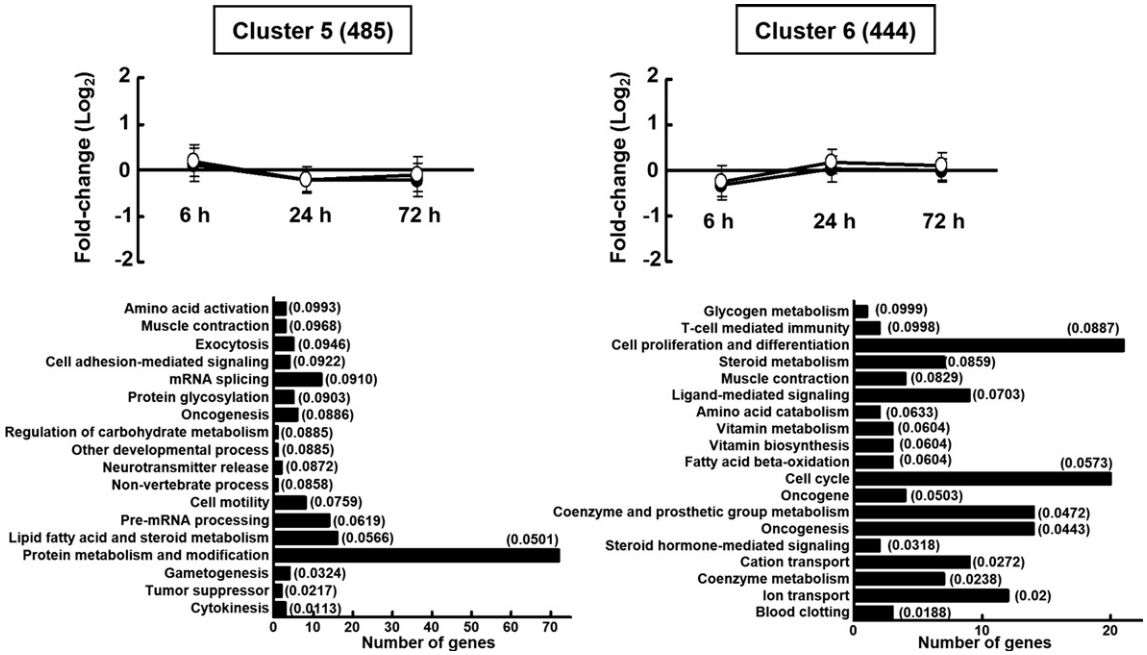


Fig. 6 (*continued*).

The biological processes related to lipid metabolism were significantly overpresented in three clusters; Cluster 1 that included up-regulated genes, Cluster 3 that included genes repressed at the early stage but recovered to control level at the late stage, and Cluster 5 that contained genes whose expression levels were maintained within relatively narrow ranges.

Next we aimed to profile the expression of genes that are associated with steatogenic hepatotoxicity as well as other biological and pharmacological functions of VPA. For the purpose, we first extracted 1156 characteristically up-regulated or down-regulated genes, of which expression changes greater than 1.5-fold with respect to the mean intensity of the time-matched control groups. The cut-off of 1.5-fold corresponded to about upper 20% of the genes with changes. Selected genes of functional importance were shown in Tables 3 and 4.

### *Expression of genes associated with lipid, fatty acid, and steroid metabolism*

Functional categorization of 1156 genes using the PANTHER revealed that 60 genes are involved in lipid, fatty acid, and steroid metabolism (Table 3). More number of genes was changed in their expression in the high-dose to compare with the low-dose, *i.e.*, 45 genes in the high-dose and 39 genes in the low-dose. Finally, we submitted 45 genes in the high-dose to the KEGG pathway database which consists of graphical diagrams of biochemical pathways, including most of the known metabolic and regulatory pathways (Ogata et al., 1999) (Fig. 7A). The results obtained from KEGG pathway analysis revealed that 10 VPA-responsive genes belonged to the biochemical pathways interconnecting four major lipid metabolic pathways, *i.e.*, glycerolipid metabolism, biosynthesis of steroids, fatty acid metabolism, and $C_{21}$-steroid hormone metabolism. Together with the fold-induction levels of each gene under treated time (Fig. 7B), we summarized that increases in lipid transport, and induction of biosynthesis of triglyceride and cholesterol at the late stage of VPA treatment may contribute to the VPA-induced steatosis in mouse liver (Table 5).

## Discussion

Drug-induced hepatotoxicity is an important healthcare issue because it causes significant morbidity and mortality, and can be extremely difficult to predict (Kaplowitz, 2001). Microarray technology is widely used for profiling the gene expression patterns induced by drugs, especially in the field of predictive toxicogenomics (Vrana et al., 2003). A comprehensive database of gene profiling that is associated with drug-induced hepatotoxicity is expected to contribute in predicting possible toxic outcomes of unknown chemicals or new drug candidates. Therefore, the Korean Toxicogenomics Research Consortium has launched a project to construct a toxicogenomics database of known hepatotoxicants. As a part of project, VPA was examined as a fatty liver-inducing drug in mouse liver by treatments with multiple doses and time points.

### *Expression patterns of genes associated with lipid, fatty acid, and steroid metabolism*

Hepatic steatosis can result from multiple abnormalities in lipid metabolism, such as increased mobilization of fatty acids coupled to increased triglyceride synthesis, or decreased secretion of triglyceride-rich lipoproteins, and impaired fatty acid oxidation (Adams et al., 2005; Portincasa et al., 2005). Although previous reports described that VPA-induced biochemical disturbances such as the inhibition of fatty acid oxidation, gluconeogenesis, ketogenesis, urea synthesis, and reduction in levels of acetyl-CoA (Becker and Harris, 1983;

Table 3
Lipid, fatty acid and steroid metabolism related genes that were altered by VPA administration[a]

| RefSeq | Gene symbol | Description | 100 mg/kg[b] | | | 1000 mg/kg[b] | | |
|---|---|---|---|---|---|---|---|---|
| | | | 6 h | 24 h | 72 h | 6 h | 24 h | 72 h |
| *Phospholipid metabolism* | | | | | | | | |
| NM_144807 | *Chpt1* | Choline phosphotransferase 1 | 0.14 | 0.45 | −0.01 | 0.29 | 0.76 | 0.05 |
| NM_028710 | *6330406P08Rik* | RIKEN cDNA *6330406P08* gene | 0.68 | −0.15 | 0.30 | 0.14 | −0.13 | 0.29 |
| NM_177730 | *1110001C20Rik* | RIKEN cDNA *1110001C20* gene | 0.11 | −0.10 | −0.17 | 0.70 | −0.06 | 0.16 |
| NM_172266 | *BC013667* | cDNA sequence BC013667 | 1.60 | 0.64 | 0.26 | 1.02 | 0.30 | 0.10 |
| NM_008149 | *Gpam* | Glycerol-3-phosphate acyltransferase, mitochondrial | −0.31 | 0.03 | 0.64 | 0.31 | 0.02 | 0.66 |
| NM_09263 | *Spp1* | Secreted phosphoprotein 1 | 0.75 | 0.47 | −0.01 | −0.32 | 0.11 | −0.34 |
| NM_018862 | *Agpat1* | 1-Acyl glycerol-3-phosphate *O*-acyltransferase 1 (lysophosphatidic acid acyltransferase, alpha) | −0.62 | −0.32 | 0.11 | −0.67 | −1.10 | 0.33 |
| NM_025576 | *2810004N20Rik* | RIKEN cDNA *2810004N20* gene | −0.59 | −0.24 | −0.36 | −0.42 | 0.05 | 0.16 |
| *Fatty acid metabolism* | | | | | | | | |
| AY037763 | *Adpn* | Adiponutrin | −0.43 | 0.35 | 1.28 | −1.14 | 0.25 | 0.93 |
| AK044017 | *Aacs* | Acetoacetyl-CoA synthetase | −0.60 | −0.30 | 0.19 | −1.99 | −0.81 | 0.55 |
| NM_019811 | *Acas2* | Acetyl-Coenzyme A synthetase 2 (ADP forming) | 0.43 | 0.37 | 0.48 | −0.09 | 0.62 | 0.75 |
| NM_007760 | *Crat* | Carnitine acetyltransferase | 0.40 | 0.57 | 0.31 | 1.72 | 0.04 | 0.10 |
| NM_198410 | *1500001B10Rik* | RIKEN cDNA *1500001B10* gene | −0.38 | −0.39 | −0.03 | 1.24 | 0.21 | 0.42 |
| NM_025802 | *0610039C21Rik* | RIKEN cDNA *0610039C21* gene | 0.59 | −0.40 | −0.05 | 0.52 | −0.01 | 0.21 |
| NM_019811 | *Acas2* | Acetyl-Coenzyme A synthetase 2 (ADP forming) | 0.43 | 0.37 | 0.48 | −0.09 | 0.62 | 0.75 |
| NM_007822 | *Cyp4a14* | Cytochrome *P*450, family 4, subfamily a, polypeptide 14 | 0.14 | 1.90 | 1.01 | 1.90 | 1.44 | 2.90 |
| NM_007703 | *Elovl3* | Elongation of very long chain fatty acids (FEN1/Elo2, SUR4/Elo3, yeast)-like 3 | 0.85 | −0.10 | −0.82 | 1.88 | 0.70 | −1.48 |
| *Cholesterol metabolism* | | | | | | | | |
| AK009261 | *Mvk* | Mevalonate kinase | −0.28 | −0.08 | 0.10 | −0.60 | 0.11 | −0.05 |
| NM_138656 | *Mvd* | Mevalonate (diphospho)decarboxylase | −0.46 | −0.21 | 0.58 | −1.23 | −0.13 | 0.38 |
| NM_010191 | *Fdft1* | Farnesyl diphosphate farnesyl transferase 1 | −0.45 | 0.30 | 0.22 | −0.61 | 0.03 | 0.08 |
| NM_020010 | *Cyp51* | Cytochrome *P*450, 51 | 0.72 | 0.71 | 0.11 | 0.21 | 0.35 | 0.04 |
| NM_018887 | *Cyp39a1* | Cytochrome *P*450, family 39, subfamily a, polypeptide 1 | 1.06 | 0.25 | −0.75 | 1.73 | −0.82 | 0.64 |
| NM_175489 | *Osbpl8* | Oxysterol binding protein-like 8 | 0.70 | −0.38 | 0.36 | −0.42 | −0.58 | 0.31 |
| NM_009890 | *Ch25h* | Cholesterol 25-hydroxylase | 0.28 | 0.50 | 0.20 | 1.22 | 0.12 | −0.23 |
| NM_025436 | *Sc4mol* | Sterol-C4-methyl oxidase-like | 0.48 | 0.59 | 0.12 | −0.56 | 0.16 | −0.22 |
| NM_008293 | *Hsd3b1* | Hydroxysteroid dehydrogenase-1, delta<5>-3-beta | −1.09 | −0.60 | 0.44 | −3.30 | −1.55 | 0.69 |
| AK088026 | *Nsdhl* | NAD(P)-dependent steroid dehydrogenase-like | 0.93 | 0.67 | −0.13 | 0.33 | 0.53 | −0.16 |
| NM_145942 | *Hmgcs1* | 3-Hydroxy-3-methylglutaryl-Coenzyme A synthase 1 | −0.06 | 1.00 | 0.49 | 0.31 | 0.23 | 0.26 |
| NM_133943 | *Hsd3b7* | Hydroxy-delta-5-steroid dehydrogenase, 3 beta- and steroid delta-isomerase 7 | −0.57 | 0.28 | −0.19 | −0.91 | 0.06 | −0.12 |
| *Lipid, fatty acid and steroid metabolism* | | | | | | | | |
| NM_007856 | *Dhcr7* | 7-Dehydrocholesterol reductase | 0.10 | 0.50 | −0.17 | 0.42 | 1.47 | 0.39 |
| NM_133815 | *Lbr* | Lamin B receptor | −0.10 | 0.05 | 0.05 | −0.63 | −0.21 | −0.41 |
| NM_009381 | *Thrsp* | Thyroid hormone-responsive SPOT14 homolog (*Rattus*) | 0.35 | −1.36 | −0.11 | −1.46 | −0.85 | −0.18 |
| *Fatty acid beta-oxidation* | | | | | | | | |
| NM_023737 | *Ehhadh* | Enoyl-Coenzyme A, hydratase/3-hydroxyacyl Coenzyme A dehydrogenase | 1.02 | 0.60 | −0.30 | 2.39 | 0.47 | 0.09 |
| *Steroid hormone metabolism* | | | | | | | | |
| NM_007809 | *Cyp17a1* | Cytochrome *P*450, family 17, subfamily a, polypeptide 1 | 0.34 | −1.04 | −0.33 | −0.20 | −0.64 | 0.37 |
| NM_134066 | *Akr1c18* | Aldo-keto reductase family 1, member C18 | −0.06 | −0.42 | −1.02 | 0.46 | 1.75 | 0.19 |
| NM_030611 | *Akr1c6* | Aldo-keto reductase family 1, member C6 | −1.01 | −0.49 | −0.01 | −0.19 | −0.14 | 0.14 |
| *Lipid metabolism* | | | | | | | | |
| NM_028943 | *4933405A16Rik* | RIKEN cDNA *4933405A16* gene | −1.32 | 0.43 | 0.18 | −0.75 | 0.51 | −0.27 |
| NM_146035 | *Mgat2* | Mannoside acetyl glucosaminyltransferase 2 | −0.21 | −0.18 | −0.20 | −0.68 | −0.10 | 0.03 |
| NM_145417 | *Rnpep* | Arginyl aminopeptidase (aminopeptidase B) | −0.12 | 0.00 | −0.31 | −0.84 | −0.13 | 0.08 |
| NM_178911 | *AI132321* | Expressed sequence AI132321 | −0.42 | −0.08 | −0.21 | −0.72 | 0.37 | 0.09 |
| NM_183191 | *MGC57096* | Hypothetical protein MGC57096 | 0.03 | −0.72 | −0.31 | −0.47 | −0.79 | 0.21 |
| *Lipid and fatty acid transport* | | | | | | | | |
| NM_011125 | *Pltp* | Phospholipid transfer protein | 0.53 | 0.81 | −0.02 | −0.15 | 1.55 | 0.26 |
| NM_153145 | *Abca8a* | ATP-binding cassette, sub-family A (ABC1), member 8a | −0.63 | 0.65 | −0.13 | −0.28 | 0.17 | 0.10 |

Table 3 (*continued*)

| RefSeq | Gene symbol | Description | 100 mg/kg [b] | | | 1000 mg/kg [b] | | |
|---|---|---|---|---|---|---|---|---|
| | | | 6 h | 24 h | 72 h | 6 h | 24 h | 72 h |
| *Lipid and fatty acid transport* | | | | | | | | |
| NM_007468 | *Apoa4* | Apolipoprotein A–IV | 0.84 | 0.26 | 0.48 | 0.06 | 0.14 | 0.32 |
| NM_008880 | *Plscr2* | Phospholipid scramblase 2 | 0.29 | 0.18 | −0.08 | −1.09 | 0.38 | −0.07 |
| NM_153389 | *Atp10d* | ATPase, Class V, type 10D | 0.68 | 0.71 | 0.39 | 0.42 | 0.32 | 1.23 |
| NM_007830 | *Dbi* | Diazepam binding inhibitor | 0.62 | 0.13 | 0.52 | 0.43 | 0.73 | 0.61 |
| NM_008375 | *Fabp6* | Fatty acid-binding protein 6, ileal (gastrotropin) | 0.94 | −0.49 | 0.26 | −0.38 | 0.15 | 0.22 |
| *Steroid metabolism* | | | | | | | | |
| NM_09994 | *Cyp1b1* | Cytochrome *P*450, family 1, subfamily b, polypeptide 1 | 1.53 | 0.08 | −0.56 | 0.60 | −0.16 | −0.35 |
| NM_028089 | *Cyp2c55* | Cytochrome *P*450, family 2, subfamily c, polypeptide 55 | −0.21 | 1.40 | 0.11 | 0.96 | 0.80 | 0.57 |
| NM_019823 | *Cyp2d22* | Cytochrome *P*450, family 2, subfamily d, polypeptide 22 | −0.22 | 0.11 | 0.02 | −1.10 | 0.44 | 0.13 |
| NM_177382 | *Cyp2r1* | Cytochrome *P*450, family 2, subfamily r, polypeptide 1 | 0.16 | 0.32 | −0.15 | −0.51 | 0.63 | −0.31 |
| NM_028979 | *Cyp2j9* | Cytochrome *P*450, family 2, subfamily j, polypeptide 9 | 0.49 | 0.92 | 0.22 | −0.11 | −0.33 | −0.55 |
| NM_009996 | *Cyp24a1* | Cytochrome *P*450, family 24, subfamily a, polypeptide 1 | −0.03 | 0.12 | 1.24 | 0.22 | −0.10 | 0.17 |
| NM_025558 | *1810044O22Rik* | RIKEN cDNA *1810044O22* gene | −0.05 | 0.95 | 0.22 | 0.17 | 0.79 | −0.04 |
| NM_024198 | *Gpx7* | Glutathione peroxidase 7 | −0.73 | −0.46 | −1.39 | −0.83 | −0.75 | −0.58 |
| *Regulation of lipid, fatty acid and steroid metabolism* | | | | | | | | |
| NM_177113 | *A830037N07Rik* | RIKEN cDNA *A830037N07* gene; peroxisome proliferative activated receptor, gamma, coactivator 1-alpha | −0.42 | −0.45 | 0.49 | −1.77 | −0.17 | −0.82 |
| NM_011480 | *Srebf1* | Sterol regulatory element binding factor 1 | −1.21 | −0.13 | −0.35 | −1.34 | −0.53 | −0.18 |
| *Other steroid metabolism* | | | | | | | | |
| NM_172769 | *Sc5d* | Sterol-C5-desaturase (fungal ERG3, delta-5-desaturase) homolog (*S. cerevisae*) | −0.63 | −0.60 | 0.12 | −0.59 | −0.59 | 0.47 |
| NM_145424 | *CRAD-L* | cis-retinol/3 alpha-hydroxysterol short-chain dehydrogenase-like | −0.65 | −0.19 | −0.07 | −0.79 | −0.23 | 0.51 |

[a] Results are expressed as the average ratio from three individual livers of the VPA-treated group and vehicle-treated control group and restricted set of 1.5-fold up-regulated or down-regulated for at least on time point in average of three mice.
[b] Data represent fold-changes on $\log_2$ scale compared to corresponding vehicle control.

Coude et al., 1983; Turnbull et al., 1985), systematic analysis to identifying the toxicity mechanism has not been approached.

Functional categorization of the VPA-altered genes using the PANTHER revealed that 60 genes are involved in lipid, fatty acid, and steroid metabolism (Table 3). Further submission of these genes to the KEGG pathway database revealed that 10 genes are closely associated with the biochemical pathways interconnecting four major lipid metabolic pathways, *i.e.*, glycerolipid metabolism, biosynthesis of steroids, fatty acid metabolism, and $C_{21}$-steroid hormone metabolism (Fig. 7). Notably, VPA induced changes in the expression of genes in the biosynthetic pathways of both triacylglycerol and cholesterol. *Gpam* and *Agpat1*, of which products acylate glycerol-3-phosphate and 1-acyl-glycerol-3-phosphate, respectively, increased in their expression, especially at 72 h of high-dose (Fig. 7). The expression of *Agpat1* has been well correlated with triglyceride synthesis (Ruan and Pownall, 2001; Gangar et al., 2002). Also genes associated with several steps in cholesterol biosynthesis were altered by VPA treatment. These genes include *Mvk* and *Mvd*, which are involved in the conversion of mevalonate into isoprene units, *Fdft1*, which catalyzes formation of squalene from farnesyl-pyrophosphate, and *Sc5d* and *Dhcr7*, which are involved in the processing of lathosterol to cholesterol. The expression of *Mvd*, *Sc5d* and *Dhcr7* was increased at 72 h with high-dose treatment. Together, this result suggests that increase of these genes in biosynthesis of triglyceride and cholesterol at the late stage may be tightly associated with the VPA-induced steatosis. However, expression of several genes in these pathways, such as *Agpat1*, *Mvd*, *Sc5d*, and *Dhcr7*, were significantly repressed at an early stage. Since VPA itself is a short-chain fatty acid, a negative feedback mechanism induced by non-physiologically high concentrations of VPA administered may induce transient repression of gene expression in the biosynthetic pathways at early stage.

Unexpectedly, expression of genes associated with fatty acid degradation was increased by VPA treatment (Table 3 and Fig. 7). *Ehhadh*, which mediates fatty acid β-oxidation, was up-regulated at 6 h and recovered to control level at 72 h. The result was largely in contrast with the previous reports that steatogenic chemicals inhibited fatty acid β-oxidation or repressed expression of genes in this process (Richards et al., 2004, Guruge et al., 2006, Yin et al., 2006). VPA may induce the genes in fatty acid β-oxidation since it is a substrate for the β-oxidation enzyme complex (Bjorge and Baillie, 1991). Therefore, the increase of *Ehhadh* expression may be unique to the VPA-induced fatty liver. Marked up-regulation of the expression of the fatty acid ω-hydroxylase gene, *Cyp4a14*, was observed throughout the entire experimental period. *Cyp4a14* is a downstream target gene of PPARα, a master regulator of adipogenesis, and is overexpressed under conditions of microvesicular steatosis and steatohepatitis (Kroetz et al., 1998; Reddy, 2001). Expression of *Adpn*, of which product transforms triacylglycerol to fatty acids, was down-regulated at 6 h, also indicating that fatty acid metabolism is inhibited by VPA at early stage (Table 3 and Fig. 7). In addition, expression of 4 genes associated with lipid and fatty acid transport, *Atp10d*, *Plscr2*, *Pltp*, and *Dbi*, was significantly changed, indicating that the

Table 4
Genes associated with known biological and pharmacological function of VPA [a]

| RefSeq | Gene symbol | Description | 100 mg/kg | | | 1000 mg/kg | | |
|---|---|---|---|---|---|---|---|---|
| | | | 6 h | 24 h | 72 h | 6 h | 24 h | 72 h |
| *Oncogenesis* | | | | | | | | |
| Oncogene | | | | | | | | |
| NM_019732 | *Runx3* | Runt-related transcription factor 3 | −0.40 | −0.49 | 0.12 | −1.65 | −0.72 | −0.21 |
| NM_008552 | *Mas1* | MAS1 oncogene | −1.71 | 1.20 | −0.18 | −1.85 | 0.68 | −0.26 |
| NM_007961 | *Etv6* | Etsvariant gene 6 (TEL oncogene) | −0.78 | 0.24 | −0.40 | −0.44 | −0.01 | 1.32 |
| NM_057173 | *Lmo1* | LIM domain only 1 | 0.06 | 1.32 | 0.28 | 0.94 | 0.88 | 0.42 |
| Oncogenesis | | | | | | | | |
| NM_019483 | *Smad9* | MAD homolog 9 (*Drosophila*) | −0.16 | −0.17 | 0.14 | −1.27 | 1.00 | 2.29 |
| BC052408 | *Fscn1* | Fascin homolog 1, actin bundling protein (*Strongylocentrotus purpuratus*) | −0.87 | 0.02 | 0.03 | −1.20 | −0.28 | −0.03 |
| NM_026018 | *Map17* | Membrane-associated protein 17 | −1.45 | −0.22 | −0.08 | −1.45 | 0.42 | −0.22 |
| Tumor suppressor | | | | | | | | |
| NM_013586 | *Loxl3* | Lysyl oxidase-like 3 | -1.08 | -0.30 | -1.09 | −1.44 | −0.43 | −0.70 |
| NM_011919 | *Ing1* | Inhibitor of growth family, member 1 | −0.43 | −0.23 | 0.64 | −1.72 | −0.03 | 0.47 |
| NM_207176 | *Tes* | Testis-derived transcript | −1.05 | −0.08 | 0.08 | −0.06 | −0.18 | 1.00 |
| *Apoptosis* | | | | | | | | |
| Apoptosis | | | | | | | | |
| NM_145392 | *Bag2* | Bcl2-associated *athanogene 2* | −1.24 | −0.57 | −0.31 | −0.25 | −0.47 | −0.39 |
| NM_008655 | *Gadd45b* | Growth arrest and DNA-damage-inducible 45 beta | 0.03 | −0.38 | −0.07 | 1.56 | 0.14 | −0.01 |
| AK085152 | *Casp9* | Caspase 9 | −0.54 | −0.05 | −0.17 | −1.40 | −0.35 | −1.36 |
| NM_009812 | *Casp8* | Caspase 8 | 0.84 | 0.31 | −0.68 | 1.02 | 0.71 | −0.60 |
| Induction of apoptosis | | | | | | | | |
| NM_013693 | *Tnf* | Tumor necrosis factor | -0.88 | -0.33 | 1.11 | -0.01 | −0.37 | 0.26 |
| NM_007828 | *Dapk3* | Death-associated kinase 3 | −1.07 | −0.73 | −0.30 | −0.69 | 0.02 | −0.23 |
| NM_008506 | *Lmyc1* | Lung carcinoma *myc*-related oncogene 1 | −0.78 | −0.98 | 0.02 | −2.22 | −0.35 | 0.25 |
| NM_023326 | *Bmyc* | Brain-expressed myelocytomatosis oncogene | −0.17 | −0.38 | −0.44 | −0.74 | 0.30 | −1.23 |
| Inhibition of apoptosis | | | | | | | | |
| NM_010900 | *Nfatc2ip* | Nuclear factor of activated T-cells, cytoplasmic, calcineurin-dependent 2 interacting protein | 1.16 | −0.46 | 0.39 | 1.17 | −0.09 | 0.23 |
| NM_009688 | *Birc4* | Baculoviral IAP repeat-containing 4 | −0.43 | −1.23 | −0.74 | −0.31 | −0.57 | 0.09 |
| NM_011361 | *Sgk* | Serum/glucocorticoid-regulated kinase | −0.63 | −0.35 | −0.19 | −1.18 | −0.44 | −0.76 |
| *Nucleoside, nucleotide and nucleic acid metabolism* | | | | | | | | |
| Chromatin packaging and remodeling | | | | | | | | |
| NM_172860 | *Cbfa2t2h* | Core-binding factor, runt domain, alpha subunit 2, translocated to, 2 homolog (human) | −0.80 | −0.03 | 0.30 | −1.67 | 0.33 | 0.61 |
| NM_198617 | *AW212607* | Expressed sequence AW212607 | −0.79 | −0.75 | −1.46 | −1.61 | −1.76 | −0.55 |
| NM_011418 | *Smarcb1* | SWI/SNF-related, matrix associated, actin-dependent regulator of chromatin, subfamily b, member 1 | −0.11 | −0.56 | −0.99 | 0.05 | −0.06 | 0.00 |
| NM_054045 | *Hist2h3c2* | Histone 2, H3c2 | −0.31 | −0.35 | 0.28 | −1.62 | −0.47 | −0.33 |
| NM_054054 | *Brdt* | Bromodomain, testis-specific | −1.13 | −0.06 | −0.55 | −0.80 | −0.23 | −0.40 |
| NM_028083 | *Chaf1b* | Chromatin assembly factor 1, subunit B (p60) | −0.23 | 0.33 | 0.67 | 2.07 | 0.76 | 0.31 |
| mRNA transcription regulation | | | | | | | | |
| NM_019563 | *Cited4* | Cbp/p300-interacting transactivator, with Glu/Asp-rich carboxy-terminal domain, 4 | -1.01 | -1.02 | -0.12 | −1.31 | −0.63 | 0.30 |
| NM_009331 | *Tcf7* | Transcription factor 7, T-cell-specific | 1.17 | 0.58 | 1.52 | 0.88 | 0.48 | 0.41 |
| NM_011850 | *Nr0b2* | Nuclear receptor subfamily 0, group B, member 2 | −2.70 | −0.97 | −0.02 | −0.94 | −1.05 | −0.09 |
| NM_013833 | *Rax* | Retina and anterior neural fold homeobox | 0.03 | 1.31 | 0.18 | −0.10 | 1.19 | 0.25 |
| NM_009322 | *Tbr1* | T-box brain gene 1 | 0.56 | 0.40 | 1.20 | 0.31 | −0.42 | 0.23 |
| NM_022409 | *Zfp296* | Zinc finger protein 296 | 0.44 | −0.50 | 1.46 | 0.08 | 1.03 | −0.33 |
| M69293 | *Idb2* | Inhibitor of DNA binding 2 | 0.86 | 0.50 | 0.19 | 1.26 | 0.47 | 0.24 |
| *Developmental processes* | | | | | | | | |
| Angiogenesis | | | | | | | | |
| NM_010516 | *Cyr61* | Cysteine-rich protein 61 | −1.52 | −0.24 | −0.06 | −1.09 | 0.43 | 0.02 |
| NM_021901 | *Tlx1* | T-cell leukemia, homeobox 1 | −1.05 | −0.43 | −0.33 | −0.57 | −0.48 | −0.17 |
| Developmental processes | | | | | | | | |
| NM_009524 | *Wnt5a* | wingless-related MMTV integration site 5A | −0.77 | −1.03 | −0.08 | −0.41 | −0.21 | 0.22 |

Table 4 (*continued*)

| RefSeq | Gene symbol | Description | 100 mg/kg | | | 1000 mg/kg | | |
|---|---|---|---|---|---|---|---|---|
| | | | 6 h | 24 h | 72 h | 6 h | 24 h | 72 h |
| *Developmental processes* | | | | | | | | |
| Fertilization | | | | | | | | |
| NM_015785 | *Zpbp* | Zona pellucida binding protein | 0.10 | 1.06 | 0.14 | 0.02 | -0.20 | -0.43 |
| Neurogenesis | | | | | | | | |
| NM_032002 | *Nrg4* | Neuregulin 4 | 1.14 | −0.53 | −0.17 | −0.72 | −0.07 | −0.16 |
| *Cell proliferation and differentiation* | | | | | | | | |
| AK042562 | *Prkcz* | Protein kinase C, zeta | −1.33 | −0.60 | −0.58 | −0.28 | 0.00 | −0.30 |
| NM_011832 | *Insrr* | Insulin receptor-related receptor | 1.23 | −0.60 | 0.28 | −0.07 | −0.35 | −0.16 |
| NM_010513 | *Igf1r* | Insulin-like growth factor I receptor | 0.15 | −0.56 | −0.06 | −1.35 | −0.86 | 0.61 |
| NM_011548 | *Tcfe2a* | Transcription factor E2a | 0.12 | −1.04 | −0.34 | −0.88 | −0.03 | 1.08 |
| NM_007631 | *Ccnd1* | Cyclin D1 | −0.81 | −1.23 | −0.57 | −0.30 | −1.24 | 0.11 |
| NM_010104 | *Edn1* | Endothelin 1 | −0.12 | 1.03 | 0.45 | 0.30 | 1.10 | 0.58 |
| NM_020013 | *Fgf21* | Fibroblast growth factor 21 | 0.80 | −0.43 | 1.01 | 4.01 | −0.94 | 3.34 |
| NM_010554 | *Il1a* | Interleukin 1 alpha | 0.35 | 0.69 | 0.00 | −1.19 | 0.04 | −0.91 |
| *Signal transduction* | | | | | | | | |
| Cell adhesion-mediated signaling | | | | | | | | |
| NM_173379 | *Leprel1* | Leprecan-like 1 | −2.19 | −0.55 | 0.02 | −1.41 | −0.59 | −0.01 |
| NM_009842 | *Cd151* | CD151 antigen | −0.95 | −1.26 | −0.37 | 0.61 | −0.36 | 0.72 |
| NM_011857 | *Odz3* | Odd Oz/ten-m homolog 3 (*Drosophila*) | −0.42 | 0.17 | 0.15 | 1.09 | 0.10 | 1.17 |
| Cytokine and chemokine-mediated signaling pathway | | | | | | | | |
| NM_010743 | *Il1rl1* | Interleukin 1 receptor-like 1 | −0.82 | −1.04 | −0.39 | −1.73 | −0.48 | −0.62 |
| NM_018827 | *Crlf1* | Cytokine receptor-like factor 1 | 0.10 | −0.40 | 0.67 | −1.05 | −0.62 | 0.47 |
| G-protein-mediated signaling | | | | | | | | |
| NM_020490 | *Ltb4r2* | Leukotriene B4 receptor 2 | −1.06 | 0.05 | 0.35 | −0.76 | 0.40 | 0.90 |
| NM_019404 | *Avpr2* | Arginine vasopressin receptor 2 | 1.23 | 0.66 | 0.92 | 0.84 | 1.12 | 1.25 |
| NM_028493 | *Rhobtb3* | Rho-related BTB domain containing 3 | −1.39 | −0.84 | −0.56 | −0.48 | −0.70 | 0.10 |
| NM_009912 | *Ccr1* | Chemokine (C–C motif) receptor 1 | 0.05 | −0.24 | −1.58 | 0.02 | −0.54 | −0.95 |
| *Immunity and defense* | | | | | | | | |
| Stress response | | | | | | | | |
| NM_026391 | *Ppp2r2d* | Protein phosphatase 2, regulatory subunit B, delta isoform | −1.71 | −1.06 | 0.91 | −2.16 | −0.45 | 0.49 |
| *Others* | | | | | | | | |
| Proteolysis | | | | | | | | |
| AK089043 | *Cacybp* | Calcyclin binding protein | 1.52 | 0.43 | 0.91 | 0.07 | −0.12 | −0.24 |
| Biological process unclassified | | | | | | | | |
| NM_020601 | *Tbl1x* | Transducin (beta)-like 1 X-linked | −0.42 | 0.12 | −0.28 | 0.41 | 0.05 | 1.41 |

[a] Data represent fold-changes on $\log_2$ scale compared to corresponding vehicle control.

function of lipid transport system may be altered by VPA (Table 3). The phospholipid transfer protein, *Pltp*, which enhances hepatic uptake of phospholipid and cholesteryl ester from HDL (Foger et al., 1997), was up-regulated at 24 h. *Pltp* is known to play a critical role in to high-density lipoproteins metabolism, which is regulated by the liver X receptor, a master regulator of cholesterol (Cao et al., 2002). We summarized the changes of these metabolic pathways at each experimental condition in Table 5. Overall the genes in biosynthesis of cholesterol and triglyceride were up-regulated at 72 h with low-dose, and 24 h and 72 h with high-dose, which is well correlated with histopathological observations of fatty liver. However, the genes in these pathways were repressed at 6 h with both doses, under which condition histopathological changes were not observed. In contrast, the gene in ω-oxidation pathway was markedly enhanced through entire experimental periods with both doses. The genes in β-oxidation were up-regulated at early stage, but, returned to normal or were repressed. These results indicate that increases in biosynthesis of cholesterol and triglyceride may contribute to the VPA-induced hepatic steatogenesis (Table 5).

Recently, several reports have addressed the transcriptomic changes associated with hepatic steatosis induced by diverse chemical toxicants. Richards et al. (2004) reported that hydrazine induced hepatic steatosis and necrosis in mice, and altered the expression of genes that are involved in lipid peroxidation/fatty acid synthesis and transport. The expression of *Cyp4a14* and *Mvd* was up-regulated at sub-toxic doses, which is consistent with the VPA-induced steatosis in our study (Table 3 and Fig. 7). Similarly, the induction of *Cyp4a* was observed in primary cultured rat hepatocytes after treatment with tetracycline, pentanoic acid, or amiodarone (de Longueville et al., 2003). These observations support the previous notion of Robertson et al. (2001) that the induction of *Cyp4a* could be used as a marker to assess steatotic injury. Our results

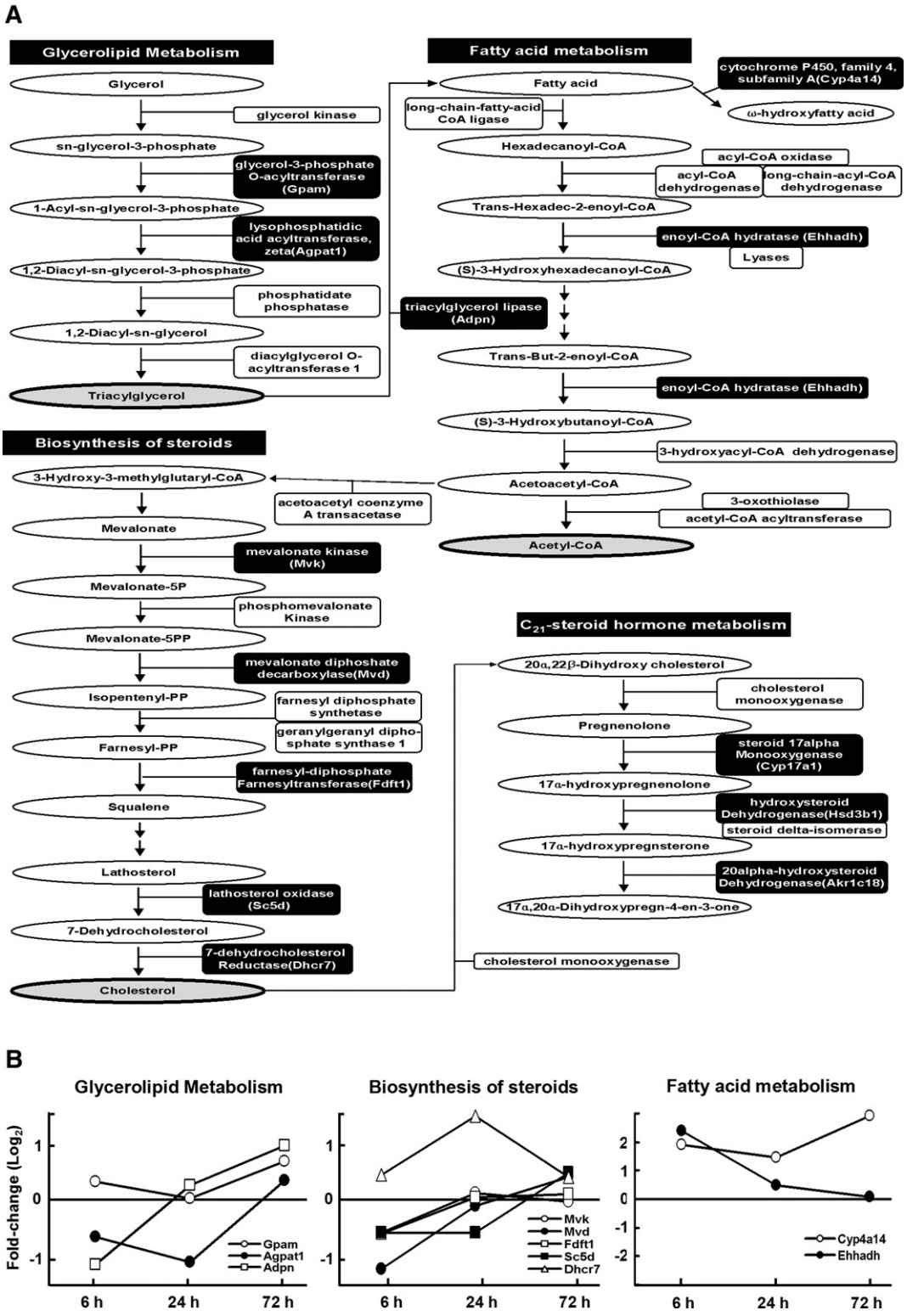


Fig. 7. KEGG pathways in lipid, fatty acid, and steroid metabolism and the related genes, the expression of which was altered by *high-dose* VPA treatment. (A) The diagram shows four interconnected KEGG pathways in lipid, fatty acid, and steroid metabolism and fourteen genes that were selected from the list in Table 3. (B) Expression levels of genes associated with the lipid, fatty acid, and steroid metabolism pathway. The *y*-axis represents the fold change in expression (VPA-treated *vs.* vehicle-treated control) on a $\log_2$ scale.

can be also compared with the carbon-tetrachloride-induced hepatic injury in rat (Chung et al., 2005). In particular, the expression of *Hsd3b1*, which is involved in steroid metabolism, was significantly up-regulated in the carbon-tetrachloride-induced fatty liver stage. The expression of the *Hsd3b1* gene was up-regulated at an early stage in our study, suggesting that

Table 5
Summary of the expression level changes of lipid metabolism-related genes by VPA [a]

| | Biological pathways | 6 h | 24 h | 72 h |
|---|---|---|---|---|
| Low-dose | Biosynthesis of triglyceride | ↓ | ↑/↓ | ↑ |
| | Biosynthesis of cholesterol | ↓ | ↑/↓ | ↑ |
| | β-Oxidation | ↑ | ↑ | ↓ |
| | ω-Oxidation | ↑ | ↑ | ↑ |
| High-dose | Biosynthesis of triglyceride | ↓ | ↑/↓ | ↑ |
| | Biosynthesis of cholesterol | ↓ | ↑ | ↑ |
| | β-Oxidation | ↑ | ↑ | – |
| | ω-Oxidation | ↑ | ↑ | ↑ |

[a] The experimental points with hepatic steatogenic changes were underlined. ↑, up-regulation and ↓, down-regulation.

steroid metabolism may be closely related to fatty liver (Table 3 and Fig. 7). The integration of these gene expression profiles responsive to diverse fatty liver-inducing chemicals would facilitate the design of a novel strategy for the prediction of hepatotoxicity through pattern recognition.

The results from our study could be compared with previous genomic studies for VPA administration. Jolly et al. (2005) performed microarray analysis with the rat livers obtained after 2000 mg/kg VPA administration and found significant changes in the biochemical pathways such as fatty acid metabolism and glycerolipid metabolism, which is consistent with our results. We found that 97 significantly altered genes were common with our results and about 20% of the overlapped genes were associated with fatty acid and steroid metabolism. Plant et al. (2002) also reported that VPA exposure in rats resulted in a significant decrease in expression of hepatic genes involved in cellular energy homeostasis such as succinate dehydrogenase, aldolase B and β-enolase by suppression subtractive hybridization. We also observed that the genes in energy homeostasis, especially cluster 3 in Fig. 3, were decreased. When rat brain was examined, alteration in lipid and glucose metabolism was observed with other signaling pathways involved in synaptic transmission and ion channels (Bosetti et al., 2005). However, studies in blood cells obtained from VPA administered patients with epilepsy, or in embryos obtained from VPA treated mice, did not show changes in lipid metabolism, suggesting that VPA may induce gene expression in a tissue-specific manner (Kultima et al., 2004; Tang et al., 2004). A contradictory observation is that Schnackenberg et al. (2006) found no changes in hepatic gene expression at 6, 12 and 24 h after a single dose of 600 mg/kg VPA to mice. Differences in the dosing protocols and/or in experimental individuals such as sex and pregnancy, might contribute to the experimental discrepancy.

### *Gene expression changes associated with other biological and pharmacological function of VPA*

VPA-induced changes in the expression of genes involved in biological processes, such as "protein metabolism and modification", "nucleoside, nucleotide, and nucleic acid metabolism" and "signal transduction" (Fig. 5). Among these, the most statistically significantly overrepresented terms included "oncogenesis" and "signal transduction" (Table 2). Table 4 showed selected genes, of which expression changes greater than 1.5-fold, with functionally categorized biological terms that are well correlated with the known biological and pharmacological functions of VPA. The fact that "oncogenesis" and related terms such as "oncogene" and "tumor suppressor" were the most significantly overrepresented terms for the VPA-regulated hepatic genes, may provide molecular mechanisms of the known chemopreventive and antitumorigenic properties of VPA (Blaheta and Cinatl, 2002; Blaheta et al., 2005). The genes in these biological processes include *Runx3*, *Mas1* and *Smad9*. VPA is known to have both pro- and anti-apoptotic characteristics in a variety of cell types and tissues (Bittigau et al., 2002; Phillips et al., 2003; Shen et al., 2005). We observed that *Casp 9* was down-regulated, whereas *Tnf* was up-regulated at a late stage, which may explain the differential apoptotic functions of VPA. The chromatin packaging and remodeling genes such as *Cbfa2t2h*, *Aw212607*, *Smarcb1* (*Snf5*), and *Cited4* were down-regulated. Down-regulation of *Smarcb1*, encoding a component of the SWI/SNF complex, was consistent with the previous report (Gresh et al., 2005). The expression of *Cyr61*, an essential regulator of vascular development (Mo et al., 2002), was down-regulated at early stage. These results indicate that the function in chromatin remodeling and angiogenesis may also be related to the anti-tumor effects of VPA.

VPA induced the expression of diverse genes associated with the major signaling pathways, such as adhesion-, cytokine- and chemokine-, and G-protein-mediated signaling pathways (Table 4). Previously it was reported that both lithium and VPA regulate GSK-3β, the inhibition of which is caused by Wnt signaling, and this event has been implicated in the morphogenesis of axons and synaptic protein clustering (Hall et al., 2002), suggesting that the Wnt signaling pathway may be closely related to the pharmacological action of VPA that targets bipolar disorders. Submission of 1156 VPA-responsive genes into KEGG revealed that 7 genes, *i.e.*, *Tcf7* (mRNA transcription regulation), *Wnt5a* (developmental process), *Prkcz* and *Ccnd1* (cell proliferation and differentiation), *Ppp2r2d* (stress response), *Cacybp* (proteolysis), and *Tblx1* (biological process unclassified) belonged to the Wnt signaling pathway, further supporting the involvement of the Wnt signaling in biological function of VPA. The genes involved in developmental processes, such as *Tlx1*, *Wnt5a*, *Zpbp* and *Nrg4*, were also altered by VPA, and this result may explain the previous finding that therapeutic doses of VPA had developmental effects, especially in the first trimester of human pregnancy (Wiltse, 2005).

In summary, we have identified and profiled the expression of genes in mouse liver after VPA administration using oligonucleotide microarray. We found that VPA regulated genes that are important in lipid transport, biosynthesis of triglyceride and cholesterol, and fatty acid oxidation. Although contributions of individual genes to the VPA-induced fatty liver require further investigation, this study provides significant insight into the mechanisms underlying VPA-mediated hepatotoxicity. Further comprehensive analysis of the gene expression profiles associated with hepatic steatosis may be a useful tool in the future for identification of potential hepatotoxicants.

## Acknowledgment

This work was supported by a Korea Food and Drug Administration grant (KFDA-05122-TGP-584).

## Appendix A. Supplementary data

Supplementary data associated with this article can be found, in the online version, at doi:10.1016/j.taap.2006.12.016.

## References

Adams, L.A., Angulo, P., Lindor, K.D., 2005. Nonalcoholic fatty liver disease. CMAJ 29, 899–905.

Becker, C.M., Harris, R.A., 1983. Influence of valproic acid on hepatic carbohydrate and lipid metabolism. Arch. Biochem. Biophys. 223, 381–392.

Bittigau, P., Sifringer, M., Genz, K., Reith, E., Pospischil, D., Govindarajalu, S., Dzietko, M., Pesditschek, S., Mai, I., Dikranian, K., Olney, J.W., Ikonomidou, C., 2002. Antiepileptic drugs and apoptotic neurodegeneration in the developing brain. Proc. Natl. Acad. Sci. U. S. A. 99, 15089–15094.

Bjorge, S.M., Baillie, T.A., 1991. Studies on the beta-oxidation of valproic acid in rat liver mitochondrial preparations. Drug Metab. Dispos. 19, 823–829.

Blaheta, R.A., Cinatl Jr., J., 2002. Anti-tumor mechanisms of valproate: a novel role for an old drug. Med. Res. Rev. 22, 492–511.

Blaheta, R.A., Michaelis, M., Driever, P.H., Cinatl Jr., J., 2005. Evolving anticancer drug valproic acid: insights into the mechanism and clinical studies. Med. Res. Rev. 25, 383–397.

Bolstad, B.M., Irizarry, R.A., Astrand, M., Speed, T.P., 2003. A comparison of normalization methods for high density oligonucleotide array data based on variance and bias. Bioinformatics 22, 185–193.

Bosetti, F., Bell, J.M., Manickam, P., 2005. Microarray analysis of rat brain gene expression after chronic administration of sodium valproate. Brain Res. Bull. 65, 331–338.

Bowden, C.L., 2003. Valproate. Bipolar Disord. 5, 189–202.

Cao, G., Beyer, T.P., Yang, X.P., Schmidt, R.J., Zhang, Y., Bensch, W.R., Kauffman, R.F., Gao, H., Ryan, T.P., Liang, Y., Eacho, P.I., Jiang, X.C., 2002. Phospholipid transfer protein is regulated by liver X receptors in vivo. J. Biol. Chem. 277, 39561–39565.

Chung, H., Hong, D.P., Kim, H.J., Jang, K.S., Shin, D.M., Ahn, J.I., Lee, Y.S., Kong, G., 2005. Differential gene expression profiles in the steatosis/fibrosis model of rat liver by chronic administration of carbon tetrachloride. Toxicol. Appl. Pharmacol. 208, 242–254.

Coude, F.X., Grimber, G., Pelet, A., Benoit, Y., 1983. Action of the antiepileptic drug, valproic acid, on fatty acid oxidation in isolated rat hepatocytes. Biochem. Biophys. Res. Commun. 115, 730–736.

de Longueville, F., Atienzar, F.A., Marcq, L., Dufrane, S., Evrard, S., Wouters, L., Leroux, F., Bertholet, V., Gerin, B., Whomsley, R., Arnould, T., Remacle, J., Canning, M., 2003. Use of a low-density microarray for studying gene expression patterns induced by hepatotoxicants on primary cultures of rat hepatocytes. Toxicol. Sci. 75, 378–392.

Foger, B., Santamarina-Fojo, S., Shamburek, R.D., Parrot, C.L., Talley, G.D., Brewer Jr., H.B., 1997. Plasma phospholipid transfer protein. Adenovirus-mediated overexpression in mice leads to decreased plasma high density lipoprotein (HDL) and enhanced hepatic uptake of phospholipids and cholesteryl esters from HDL. J. Biol. Chem. 272, 27393–27400.

Gangar, A., Raychaudhuri, S., Rajasekharan, R., 2002. Alteration in the cytosolic triacylglycerol biosynthetic machinery leads to decreased cell growth and triacylglycerol synthesis in oleaginous yeast. Biochem. J. 365, 577–589.

Gottlicher, M., Minucci, S., Zhu, P., Kramer, O.H., Schimpf, A., Giavara, S., Sleeman, J.P., Lo Coco, F., Nervi, C., Pelicci, P.G., Heinzel, T., 2001. Valproic acid defines a novel class of HDAC inhibitors inducing differentiation of transformed cells. EMBO J. 20, 6969–6978.

Gresh, L., Bourachot, B., Reimann, A., Guigas, B., Fiette, L., Garbay, S., Muchardt, C., Hue, L., Pontoglio, M., Yaniv, M., Klochendler-Yeivin, A., 2005. The SWI/SNF chromatin-remodeling complex subunit SNF5 is essential for hepatocyte differentiation. EMBO J. 24, 3313–3324.

Gunther, E.C., Stone, D.J., Gerwien, R.W., Bento, P., Heyes, M.P., 2003. Prediction of clinical drug efficacy by classification of drug-induced genomic expression profiles in vitro. Proc. Natl. Acad. Sci. U. S. A. 100, 9608–9613.

Guruge, K.S., Yeung, L.W.Y., Yamanaka, N., Miyazaki, S., Lam, P.K.S., Giesy, J.P., Jones, P.D., Yamashita, N., 2006. Gene expression profiles in rat liver treated with perfluorooctanoic acid (PFOA). Toxicol. Sci. 89, 93–107.

Gurvich, N., Tsygankova, O.M., Meinkoth, J.L., Klein, P.S., 2004. Histone deacetylase is a target of valproic acid-mediated cellular differentiation. Cancer Res. 64, 1079–1086.

Hall, A.C., Brennan, A., Goold, R.G., Cleverley, K., Lucas, F.R., Gordon-Weeks, P.R., Salinas, P.C., 2002. Valproate regulates GSK-3-mediated axonal remodeling and synapsin I clustering in developing neurons. Mol. Cell. Neurosci. 20, 257–270.

Huber, W., von Heydebreck, A., Sultmann, H., Poustka, A., Vingron, M., 2002. Variance stabilization applied to microarray data calibration and to the quantification of differential expression. Bioinformatics 18, 96–104.

Jolly, R.A., Goldstein, K.M., Wei, T., Gao, H., Chen, P., Huang, S., Colet, J.M., Ryan, T.P., Thomas, C.E., Estrem, S.T., 2005. Pooling samples within microarray studies: a comparative analysis of rat liver transcription response to prototypical toxicants. Physiol. Genomics. 22, 346–355.

Kaplowitz, N., 2001. Causality assessment versus guilt-by-association in drug hepatotoxicity. Hepatology 33, 308–310.

Kassahun, K., Abbott, F., 1993. In vivo formation of the thiol conjugates of reactive metabolites of 4-ene VPA and its analog 4-pentanoic acid. Drug Metab. Dispos. 21, 1098–1106.

Kesterson, J.W., Granneman, G.R., Machinist, J.M., 1984. The hepatotoxicity of valproic acid and its metabolites in rats: I. Toxicologic, biochemical and histopathologic studies. Hepatology 4, 1143–1152.

Kroetz, D.L., Yook, P., Costet, P., Bianchi, P., Pineau, T., 1998. Peroxisome proliferator-activated receptor alpha controls the hepatic CYP4A induction adaptive response to starvation and diabetes. J. Biol. Chem. 273, 31581–31589.

Kultima, K., Nystrom, A.M., Scholz, B., Gustafson, A.L., Dencker, L., Stigson, M., 2004. Valproic acid teratogenicity: a toxicogenomics approach. Environ. Health Perspect. 112, 1225–1235.

Lewis, J.H., Zimmerman, H.J., Garrett, C.T., Rosenberg, E., 1982. Valproate-induced hepatic steatogenesis in rats. Hepatology 2, 870–873.

Loscher, W., 1978. Serum protein binding and pharmacokinetics of valproate in man, dog, rat and mouse. J. Pharmacol. Exp. Ther. 204, 255–261.

Loscher, W., 1999. Valproate: a reappraisal of its pharmacodynamic properties and mechanisms of action. Prog. Neurobiol. 58, 31–59.

Mi, H., Lazareva-Ulitsky, B., Loo, R., Kejariwal, A., Vandergriff, J., Rabkin, S., Guo, N., Muruganujan, A., Doremieux, O., Campbell, M.J., Kitano, H., Thomas, P.D., 2005. The PANTHER database of protein families, subfamilies, functions and pathways. Nucleic Acids Res. 33, 284–288.

Mo, F.E., Muntean, A.G., Chen, C.C., Stolz, D.B., Watkins, S.C., Lau, L.F., 2002. CYR61 (CCN1) is essential for placental development and vascular integrity. Mol. Cell. Biol. 22, 8709–8720.

Ogata, H., Goto, S., Sato, K., Fujibuchi, W., Bono, H., Kanehisa, M., 1999. KEGG: Kyoto Encyclopedia of Genes and Genomes. Nucleic Acids Res. 27, 29–34.

Phillips, A., Bullock, T., Plant, N., 2003. Sodium valproate induces apoptosis in the rat hepatoma cell line, FaO. Toxicology 192, 219–227.

Ponchaut, S., van Hoof, F., Veitch, K., 1992. In vitro effects of valproate and valproate metabolites on mitochondrial oxidations. Relevance of CoA sequestration to the observed inhibitions. Biochem. Pharmacol. 43, 2435–2442.

Portincasa, P., Grattagliano, I., Palmieri, V.O., Palasciano, G., 2005. Nonalcoholic steatohepatitis: recent advances from experimental models to clinical management. Clin. Biochem. 38, 203–217.

Powell-Jackson, P.R., Tredger, J.M., Williams, R., 1984. Hepatotoxicity to sodium valproate: a review. Gut 25, 673–681.

Reddy, J.K., 2001. Nonalcoholic steatosis and steatohepatitis: III. Peroxisomal beta-oxidation, PPAR alpha, and steatohepatitis. Am. J. Physiol.: Gastrointest. Liver Physiol. 281, 1333–1339.

Richards, V.E., Chau, B., White, M.R., McQueen, C.A., 2004. Hepatic gene expression and lipid homeostasis in C57BL/6 mice exposed to hydrazine or acetylhydrazine. Toxicol. Sci. 82, 318–332.

Plant, N., Barber, P., Horner, E., Cockburn, C.L., Gibson, G., Bugelski, P., Lord, P., 2002. Differential gene expression in rats following subacute exposure to the anticonvulsant sodium valproate. Toxicol. Appl. Pharmacol. 183, 127–134.

Robertson, G., Leclercq, I., Farrell, G.C., 2001. Nonalcoholic steatosis and steatohepatitis: II. Cytochrome *P*-450 enzymes and oxidative stress. Am. J. Physiol.: Gastrointest. Liver Physiol. 281, 1135–1139.

Roma-Giannikou, E., Syriopoulou, V., Kairis, M., Pangali, A., Sarafidou, J., Constantopoulos, A., 1999. In vivo effect of sodium valproate on mouse liver. Cell. Mol. Life Sci. 56, 363–369.

Ruan, H., Pownall, H.J., 2001. Overexpression of 1-acyl-glycerol-3-phosphate acyltransferase-alpha enhances lipid storage in cellular models of adipose tissue and skeletal muscle. Diabetes 50, 233–240.

Saeed, A.I., Sharov, V., White, J., Li, J., Liang, W., Bhagabati, N., Braisted, J., Klapa, M., Currier, T., Thiagarajan, M., Sturn, A., Snuffin, M., Rezantsev, A., Popov, D., Ryltsov, A., Kostukovich, E., Borisovsky, I., Liu, Z., Vinsavich, A., Trush, V., Quackenbush, J., 2003. TM4: a free, open-source system for microarray data management and analysis. Biotechniques 34, 374–378.

Schmidt, D., 1984. Adverse effects of valproate. Epilepsia 25, 44–49.

Schnackenberg, L.K., Jones, R.C., Thyparambil, S., Taylor, J.T., Han, T., Tong, W., Hansen, D.K., Fuscoe, J.C., Edmondson, R.D., Beger, R.D., Dragan, Y.P., 2006. An integrated study of acute effects of valproic acid in the liver using metabonomics, proteomics, and transcriptomics platforms. OMICS 10, 1–14.

Searfoss, G.H., Jordan, W.H., Calligaro, D.O., Galbreath, E.J., Schirtzinger, L.M., Berridge, B.R., Gao, H., Higgins, M.A., May, P.C., Ryan, T.P., 2003. Adipsin, a biomarker of gastrointestinal toxicity mediated by a functional gamma-secretase inhibitor. J. Biol. Chem. 278, 46107–46116.

Shen, W.T., Wong, T.S., Chung, W.Y., Wong, M.G., Kebebew, E., Duh, Q.Y., Clark, O.H., 2005. Valproic acid inhibits growth, induces apoptosis, and modulates apoptosis-regulatory and differentiation gene expression in human thyroid cancer cells. Surgery 138, 979–984.

Steinley, D., 2006. *K*-means clustering: a half-century synthesis. Br. J. Math. Stat. Psychol. 59, 1–34.

Tang, Y., Glauser, T.A., Gilbert, D.L., Hershey, A.D., Privitera, M.D., Ficker, D.M., Szaflarski, J.P., Sharp, F.R., 2004. Valproic acid blood genomic expression patterns in children with epilepsy—A pilot study. Acta. Neurol. Scand. 109, 159–168.

Tong, V., Teng, X.W., Chang, T.K., Abbott, F.S., 2005. Valproic acid: I. Time course of lipid peroxidation biomarkers, liver toxicity, and valproic acid metabolite levels in rats. Toxicol. Sci. 86, 427–435.

Troyanskaya, O., Cantor, M., Sherlock, G., Brown, P., Hastie, T., Tibshirani, R., Botstein, D., Altman, R.B., 2001. Missing value estimation methods for DNA microarrays. Bioinformatics 17, 520–525.

Turnbull, D.M., Bone, A.J., Tames, F.J., Wilson, L., Baird, J.D., Sherratt, H.S., 1985. The effect of valproate on blood metabolite concentrations in spontaneously diabetic, ketoacidotic, BB/E Wistar rats. Diabetes Res. 2, 45–48.

Vrana, K.E., Freeman, W.M., Aschner, M., 2003. Use of microarray technologies in toxicology research. Neurotoxicology 24, 321–332.

Wiltse, J., 2005. Mode of action: inhibition of histone deacetylase, altering WNT-dependent gene expression, and regulation of beta-catenin—Developmental effects of valproic acid. Crit. Rev. Toxicol. 35, 727–738.

Yin, H.Q., Kim, M., Kim, J.H., Kong, G., Lee, M.O., Kang, K.S., Yoon, B.I., Kim, H.L., Lee, B.H., 2006. Hepatic gene expression profiling and lipid homeostasis in mice exposed to steatogenic drug, tetracycline. Toxicol. Sci. 94, 206–216.